journal

J. Am. Ceram. Soc., 90 [9] 2863–2867 (2007)
DOI: 10.1111/j.1551-2916.2007.01784.x

Convection Patterns in Liquid Oxide Films on ZrB_2–SiC Composites Oxidized at a High Temperature

Sigrun N. Karlsdottir and John W. Halloran†

Materials Science and Engineering Department, University of Michigan, Ann Arbor, Michigan 48109-2136

Carl E. Henderson

Department of Geological Sciences, University of Michigan, Ann Arbor, Michigan 48109-1005

During the high-temperature oxidation of ZrB_2–SiC composites, liquid boron oxide (B_2O_3) is formed at the zirconium diboride–zirconium oxide interface and transported through the overlying layer of silica liquid by convection, forming distinct convection cells arranged like the petals of a flower. The convection cells are localized by a viscous fingering phenomenon, as the fluid B_2O_3 rich liquid solution rises through the viscous silica layer. The upwelling B_2O_3 rich liquid contains dissolved zirconium dioxide, which deposits in the center of the flower-like structure as the B_2O_3 evaporates. The driving force for the B_2O_3 liquid flow is the volume increase upon oxidation of ZrB_2. Convective transport of B_2O_3 liquids suggests a novel mechanism for the high-temperature oxidation of these materials.

I. Introduction

Patterns form when a less viscous liquid displaces a more viscous liquid, a phenomenon known as viscous fingering.[1] The viscous fingers form because of the instability of the moving interface[2] between two liquids with a large viscosity contrast.[3] Viscous fingering is an important phenomenon in the formation of patterns at the nanoscale,[4] the microscale,[5] as well as macroscopic features in magma intrusions.[6] They have not yet been reported in the liquid oxide films that form during oxidation of refractory diboride materials. Here, we present horizontal patterns of boron oxide (B_2O_3)-rich borosilicate–zirconia liquids in liquid oxide films formed by oxidation of ZrB_2–silicon carbide (SiC) ultrahigh-temperature composites at 1550°C.

When exposed to air at very high temperatures, zirconium diboride reacts to form crystalline zirconium oxide and boron oxide (boria, B_2O_3),[7,8] which is a quite fluid liquid. The SiC reacts to form silicon oxide (silica, SiO_2), a very viscous liquid. Typically, a two-layer oxide film forms, with a zirconium oxide inner film and a SiO_2 outer film.[8–13] Here, our attention is directed toward the outer film. The SiO_2 can dissolve with the B_2O_3 to form a B_2O_3–SiO_2 liquid solution of intermediate viscosity. At the temperature of oxidation, B_2O_3 is much more volatile than SiO_2.[7,9,12,13] At the outer surface of the oxide, the B_2O_3 is preferentially evaporated, so that the liquid film at the outer surface is predominantly viscous SiO_2. Microstructural evidence suggest that Oxygen (O) is transported inward through the oxide film, to react at the interface between the oxide and the boride. The convection patterns we report here suggests that a more fluid boria-rich B_2O_3–SiO_2 liquid formed underneath the oxide film flows outward through the viscous silica-rich film, undergoing viscous fingering instability. The fluid liquid emerges through the film and flows laterally on the outside film surface. As B_2O_3 evaporates at the oxide surface, the remaining liquid is viscous SiO_2.

II. Experimental Procedure

The UHTC material, ZrB_2–15 vol% SiC, used in this work was fabricated and provided by CNR-ISTEC (The Institute of Science and Technology for Ceramics, National Research Council, Faenza, Italy). Details of the properties and processing are presented in more detail elsewhere.[14] Specimens tested were rectangular prisms with an average surface area of 1 cm^2. Oxidation was conducted in ambient laboratory air by heating to 1550°C at a heating rate of 13°C/min and free cooling with dwelling times of 1.5, 2, and 4 h in a conventional furnace (Lindberg, Watertown, WI). The specimens were supported on pieces of the same material. Before testing, the specimen was ultrasonically cleaned in acetone and dried. The specimen was stored in moisture free desiccators after testing. A cross section of the oxidized specimen was prepared for microstructural analysis by nonaqueous polishing procedures down to 0.5 μm finish. The composition and morphology of the oxide scale formed after the oxidation test was characterized by scanning electron microscopy (SEM), backscattering electron microscopy (BSE), and X-ray energy dispersive spectroscopy (XEDS). Electron microprobe analysis (EMPA) was performed on the surfaces of the specimen by using well-characterized mineral standards for qualitative analysis of boron (B), O, zirconium (Zr), and silicon (Si) with Cameca SX100 (Cameca, Gennevilliers, France), which was also used for imaging in the BSE and cathodoluminscence (CL) modes. The standards used for each element were as follows: PC3 (200 Å) for B, LPC0 (46 Å) for O, PET (8.75 Å) for Zr, and TAP (25.7 Å) for Si. The CL detector used is panchromatic, which collects visible light (~400–700 nm) given off by the sample when impacted by the electron beam. The EMPA X-ray maps were acquired using a 10 keV, 40 nA electron beam with a 40 μs pixel dwell time and were background corrected by image subtraction of a second map acquired with the spectrometer set to a nearby off-peak position to avoid any false counts for B due to the high X-ray background in the Zr mapping. Specimens were coated with C before microstructural and elemental analysis. Analyses were performed on the surface of the specimens and cross sections.

III. Results and Discussion

(1) Microstructure Observation Related to Convection

Mass transport by liquid convection has not yet been reported for high-temperature oxidation, but the microstructure of the oxide films on this material shows clear evidence of liquid flow. Figure 1(a) shows a backscattered electron image (BSE) of the surface of a sample oxidized for 2 h at 1550°C. Notice the

N. Jacobson—contributing editor

Manuscript No. 22739. Received January 28, 2007; approved April 10, 2007.
†Author to whom correspondence should be addressed. e-mail: peterjon@umich.edu

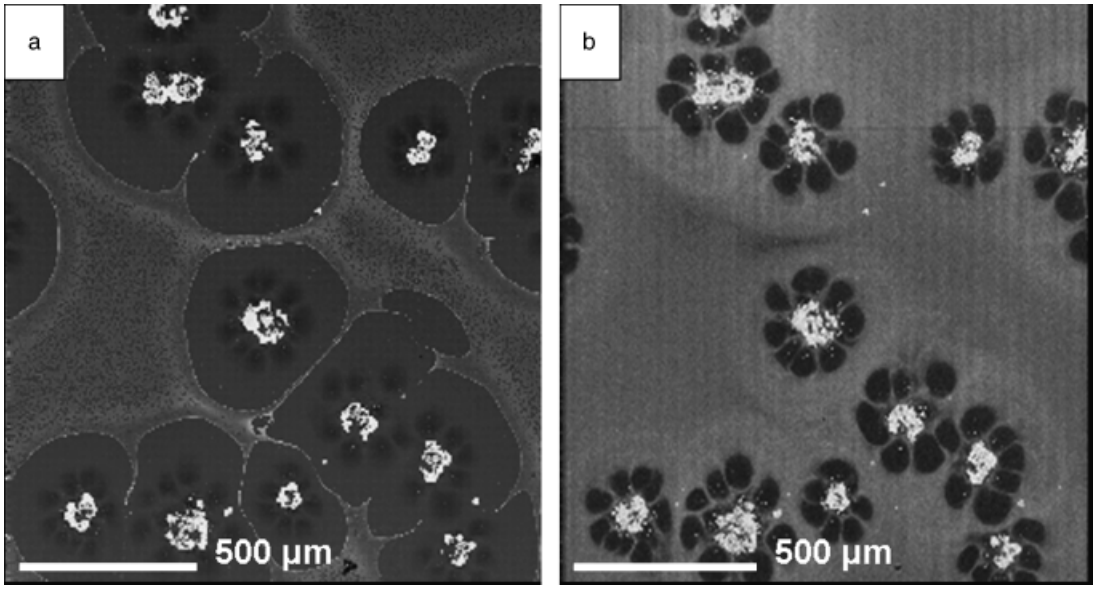

Fig. 1. (a) Features on the surface of sample oxidized 2 h at 1550°C, imaged in backscattered electrons. Bright features are zirconium oxide, surrounded by a ca. 300 μm region in darker contrast, which is silica glass (which was liquid at 1550°C). The areas of brighter contrast consist of micron-size zirconium oxide particles. (b) Same area shown in (a) imaged by cathodoluminescence. The flower-like patterns that have lobes in dark contrast are shown by electron probe microanalysis to be rich in boron oxide, while the areas in light gray contrast are silicon oxide.

island-in-lagoon patterns. EMPA showed that the bright island-like features consist of zirconium oxide, while the dark-gray lagoon-like regions are mostly silicon dioxide. The medium-gray regions outside of the lagoons are silicon dioxide decorated with many small particles of zirconium oxide. Figure 1(b) is imaged using CL imaging. The flower-like patterns revealed by CL have lobes in dark contrast, which are shown by electron probe microanalysis to be rich in B_2O_3, while the area in light-gray contrast are SiO_2. These are apparently convection cells of borate-rich borosilicate liquid surrounding an emergent zirconium oxide column. Figure 2 shows EPMA line analysis performed on one of the convection cells on a specimen oxidized for 4 h at 1550°C. The X-ray intensity (counts per second (cps)) vs. location in the oxide scale (μm) is shown for B, O, Zr, and Si. The start of the line is labeled with A (i.e., 0 μm) and the end with B (i.e., 300 μm). From Fig. 2, the increase in B where the line crosses the pedals is evident. The line analyses also show that the middle part of the cell mainly contains zirconia (ZrO_2).

We suggest that the lagoon-like features are created by borosilicate liquid moving radially across the surface from the central ZrO_2 column. B_2O_3 subsequently evaporates near the surface, leaving a viscous silica-rich surface layer. The silica-rich regions outside of the lagoon-like features are decorated with many small particles of zirconium oxide. This is shown in Fig. 3(a), where the black arrows point out swirls of small zirconium oxide particles on a surface of a specimen oxidized for 4 h at 1550°C. This is shown in more detail in Fig. 3(b), where the swirling arrangement of the small particles suggests that they were carried by a flowing liquid. Figure 4 shows a BSE image of a cross section through the middle of a convection cell on the specimen oxidized for 4 h at 1550°C. The image shows the emergent zirconium oxide column in the middle of the convection cell sur-

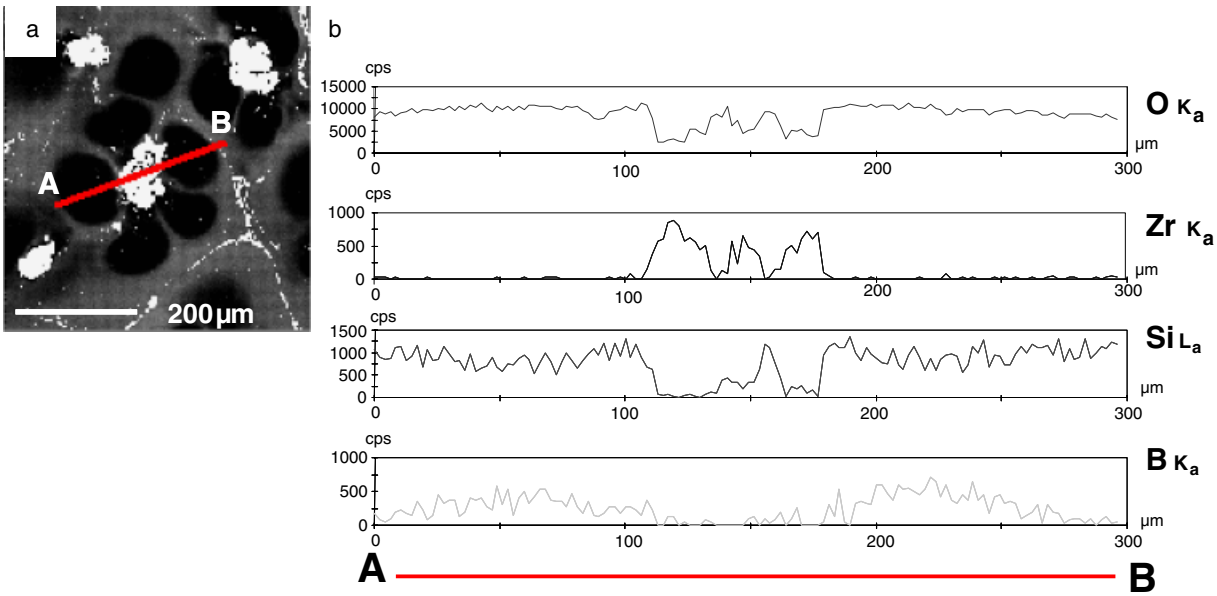

Fig. 2. Line analysis on electron microprobe analyzing maps (a) backscattered electrons image of a cell on surface of a ZrB_2–15 vol% silicon carbide composite tested at 1550°C for 4 h. The red line through the cell indicates where the intensity of the elements was recorded, where letter A indicates the start of the line scan and B the end (b) graphs of the recorded intensity (counts per second (Cps)) versus distance (μm) of the line scan shown in (a).

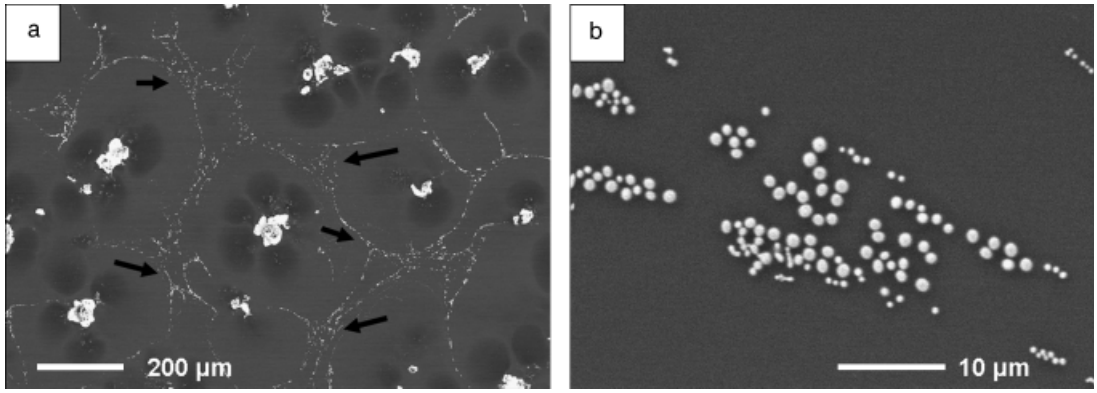

Fig. 3. Surface of a sample oxidized at 1550°C for 4 h (a) backscattered electrons image of clusters of particles in pattern suggestive of flow; the black arrows indicate the clusters of the zirconium oxide particles, (b) detail of the 0.5–2 μm zirconium oxide particles.

rounded by borosilicate glass as well as having some more B_2O_3-rich liquid in the middle of the ZrO_2. The formation of the zirconium oxide deposits found in the center of the convection cells during the oxidation is reported in detail elsewhere[15] where calculated phase equilibrium diagrams and microstructure observations are used for interpretation.

The convection cells are associated with surface topography. Figure 5(a) shows an SEM image of a surface oxidized for 1.5 h at 1550°C tilted at an angle to emphasize topography. This area has four neighboring convection cells, with the side lobes visible in the BSE in Fig. 5(b). The secondary electron image in Fig. 5(a), which does not have contrast for the ZrO_2 or the B-rich lobes, shows the central ZrO_2 column rising above the film surface, with what appears to be elevated regions between the convection cells. Many bumps on the silicate surface are obvious, which could be convection cells that have yet to emerge on the surface.

(2) Convection Mechanism

We presume that the localized convection cells with the convection patterns arise through vertical viscous fingering, where the fluid borosilicate flows through a more viscous silica-rich fluid. The side lobes are believed to be a lateral finger pattern. The viscosity variation with B/Si ratio in borosilicate liquids is extreme. At 1550°C, the viscosity of silica is on order 100 GPa · s, while B_2O_3 has a viscosity of only about 40 Pa · s. Extrapolating from the data of Jabra *et al.*,[16] we can roughly estimate the dependence of viscosity with mole fraction B_2O_3 ($X_{B_2O_3}$) at 1550°C as $\log_{10}\eta = 11 - 9X_{B_2O_3}$.

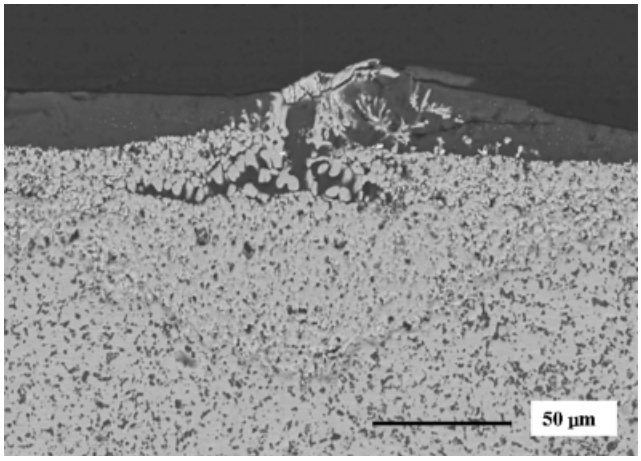

Fig. 4. Backscattered electrons image of a cross section through the middle of a convection cell on the specimen oxidized for 4 h at 1550°C. The image shows the emergent zirconium oxide column in the middle of the convection cell surrounded by borosilicate glass as well as having some more boron oxide-rich liquid in the middle of the ZrO_2.

We assume that at steady state, the composition of the freshly formed oxides (crystalline ZrO_2 and liquid B_2O_3–SiO_2 solution) at the boride/oxide interface is roughly in the ratio expected for oxidation of 85 vol% ZrB_2–15 vol% SiC (or 79 mole% ZrB_2). The composition of fresh oxide liquid solution should be around

$$X_{B_2O_3} = 0.79\,B_2O_3$$

The viscosity at this composition should be about 1000 Pa · s. B_2O_3 is much more volatile than silica. B_2O_3 has a vapor pressure of 233 Pa at 1500°C, compared with a vapor pressure of 3×10^{-4} Pa for silica.[9] At the surface, where the B_2O_3 can evaporate, there should be a silica-rich liquid surface layer with essentially no remaining B_2O_3 in solution. This silica-rich surface layer should have a viscosity around 10–100 GPa · s. The viscosity ratio V_R between the viscous surface layer and the fluid fresh oxide liquid would be very large indeed, ca. $V_R = 10^6$–10^7. This large viscosity ratio should enable quite thin viscous fingers to form.

The convection is not forced by density differences, because similar features are observed on the upward-facing, side-facing, and downward-facing surfaces of the samples.[15] Rather, we suggest that the driving force for borate flow is the very large volume increase upon oxidation of ZrB_2. The molar volume of the condensed oxides is different than the molar volume of the substrate. In the literature for oxidation of metals, the oxide/metal volume ratio is known as the Pillings–Bedworth Ratio (PBR). When the SiC is oxidized to silicon dioxide, the molar volume of SiC (12.47 cm^3/mole) is much smaller than the molar volume of SiO_2 (27.43 cm^3/mole). The carbon oxidizes to CO gas. The ratio of the molar volume of silica to the molar volume of SiC is the PBR of SiO_2 PBR_{SiO_2}, which is 2.2. For ZrB_2, we can define partial PBRs for B and for Zr, and a total PBR, using the molar volumes of ZrB_2 (18.54 cm^3/mole), B_2O_3 (55.2 cm^3/mole),[17] and ZrO_2 (20.92 cm^3/mole). The B partial PBR_B is 2.98, forming a liquid that can flow. The zirconium partial PBR_Z is 1.13, with the zirconium oxide being a rigid solid. Combining the liquids formed from the 85 vol% ZrB_2−15 vol% SiC, 1 unit volume of UHTC upon oxidation produces 0.96 unit volumes of solid oxide and 2.8 unit volumes of liquid oxide, for an overall 380% volume increase. The liquid oxide must be *squeezed up* away from the interface. It is likely that the volume increase upon oxidation is the driving force for liquid flow. A schematic of the proposed mechanism is shown in Fig. 6. The proposed mechanism for the development of the viscous fingering of the B_2O_3-rich liquid going through the viscous outer silica during oxidation is demonstrated in Fig. 6(d). BSE and CL images (Figs. 6(a) and (b)) of a surface of a sample oxidized for 2 h at 1550°C are also shown in Fig. 6 as well as EMPA elemental map showing the distribution of B (Fig. 6(c)). The white areas on the

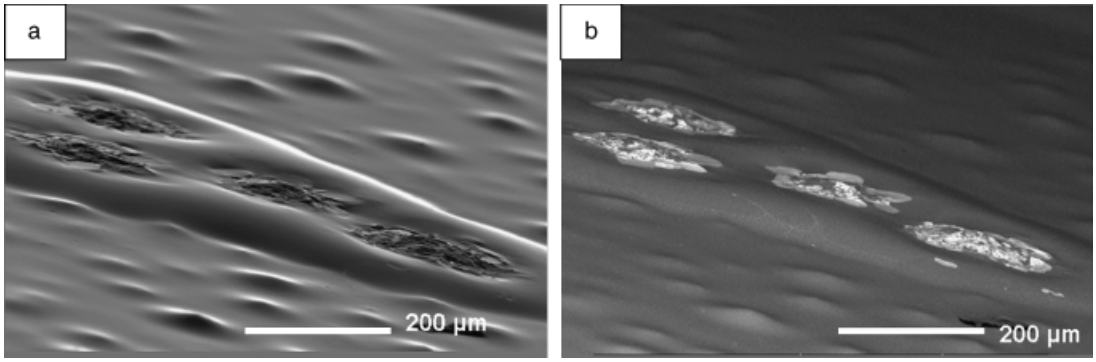

Fig. 5. Surface of sample oxidized 1550°C for 1.5 h, viewed from an angle to reveal surface topography (a) scanning electron microscopy image where surface topography is more obvious, (b) backscattered electrons image of the same surface area where the boron-rich lobes are imaged.

map indicate a higher intensity of $K\alpha$ X-rays detected for B, while the black region presents zero detected intensity of B.

(3) Role of Convection on Zirconium Diboride Composite Oxidation

Composites of zirconium diboride and SiCs are prominent members of the class of ultrahigh temperature ceramics now receiving attention for very high-temperature applications.[10] Their oxidation behavior is well-known.[8–13] The ZrB_2 forms ZrO_2 and B_2O_3 in direct contact with the diboride, while SiO_2 (and CO) forms by oxidation of SiC deeper into the material. Over the zirconium diboride grows a layer of columnar zirconium oxide with glass between the layers, which is covered with a glassy outer layer consisting of SiO_2 and B_2O_3. Depending on the temperature and oxidation conditions, some or all of these features are commonly observed.

It has been well appreciated that the glass at the oxidation temperature is liquid, and is greatly depleted in B_2O_3 because much of the volatile B_2O_3 evaporates during oxidation.[7,12] Lateral flow of liquid has been described for some B_2O_3-forming materials.[18,19] However, convective flow of B_2O_3–SiO_2 liquids has not been recognized as a major transport mechanism. Here, we argue that the mechanism of formation of the outer silicate layer is the result of the upwelling of borosilicate liquids through convection cells, with subsequent lateral flow over the outer surface. The outer SiO_2 layer forms as a residue of this liquid, after evaporation of the B_2O_3. This outer silicate layer is believed to be very important for oxidation resistance, as it forms a passive layer that slows oxidation. The loss of the silicate layer at higher temperatures (where silica itself is vola-

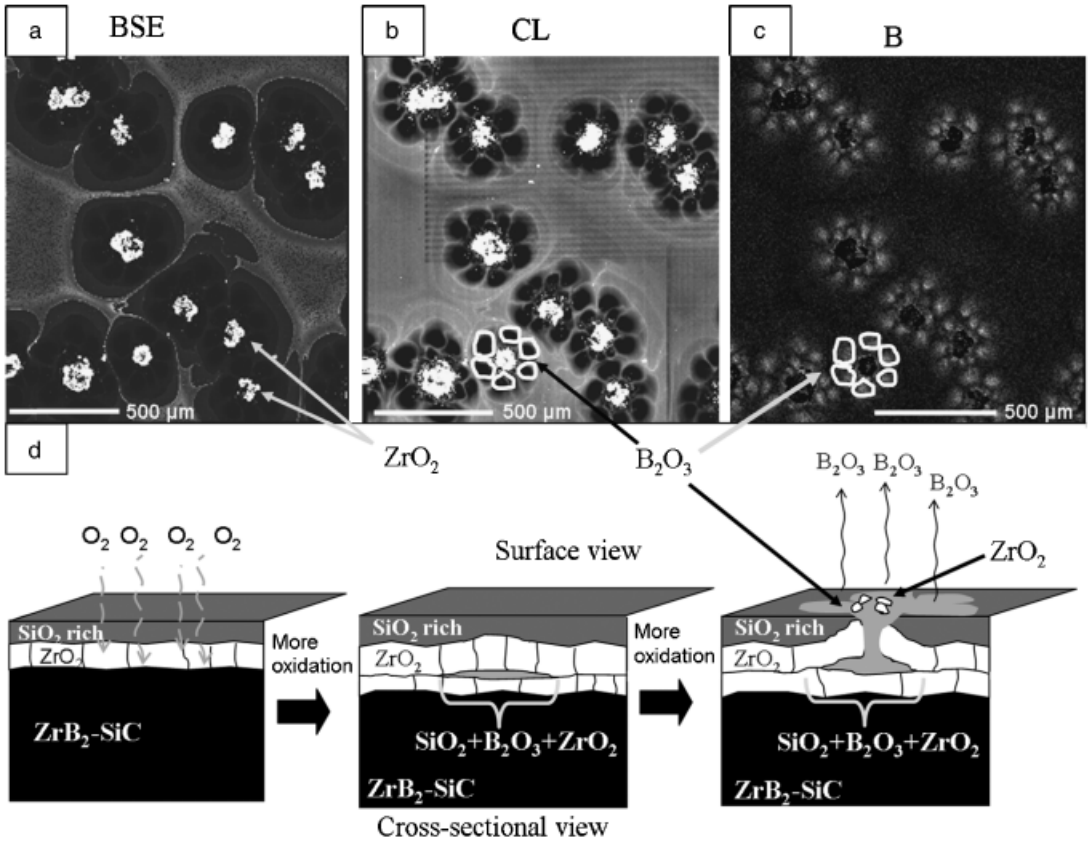

Fig. 6. (a) Backscattered electrons (BSE) and (b) cathodoluminscence (CL) images of a sample oxidized for 2 h at 1550°C, (c) electron microprobe analyzing (EMPA) elemental map of the same area as in (a) and (b), showing the distribution of boron (B). The white color indicates higher intensity of $K\alpha$ X-rays detected for B, while the black region presents zero intensity. (d) Schematic of the proposed mechanism showing the development of the viscous fingering of the boron oxide-rich liquid going through the viscous outer silica liquid oxide during oxidation.

tile) results in much faster active oxidation.[13] Maintaining a passivating layer of silicate liquid requires a balance of processes that diminish the layer, such as silicate vaporization, with processes that replenish the layer. If replenishment indeed occurs by borosilicate convection, the convection patterns reported here can play a critical role providing oxidation resistance at a high temperature.

IV. Conclusions

We observe island-in-lagoon patterns on oxide scales formed by oxidation of a ZrB_2–SiC composite exposed to air at 1550°C, consisting of a central zirconia "island" in a silica-rich "lagoon." Within the latter is a pattern of B_2O_3 rich lobes, arranged like flower petals. We interpret these features as convection cells transporting a fluid liquid boria-rich borosilicate oxidation product to the surface where B_2O_3 is lost by evaporation, depositing zirconia in a viscous silica-rich liquid, forming the island-in-lagoon pattern. The driving force for transport is the large volume increase upon oxidation. The boria-rich flower patterns are formed by a viscous fingering process as fluid boria–silica–zirconia liquid displaces the more viscous silica-rich liquid. The process of convective transport of liquid oxide solution, with evaporation of B_2O_3 and deposition of ZrO_2 in viscous silica liquid, is the mechanism of formation of the external silica scales observed on ZrB_2–SiC composites.

Acknowledgments

The authors thank Alida Bellosi and her associates at CNR-ISTEC in Italy for providing the ZrB_2–SiC materials. We thank The Office of Naval Research for financial support under the grant N0014-02-1-0034, and the National Science Foundation for funding the electron microprobe under EAR-9911352.

References

[1]P. G. Saffman and G. Taylor, "Penetration of a Fluid Into a Porous Medium or Hele-Shaw Cell Containing a More Viscous Liquid," *R. Soc. [London] Proc. Ser. A*, **245** [1242] 312–29 (1958).

[2]J. S. Langer, "Dendrites, Viscous Fingers, and the Theory of Pattern Formation," *Science*, **243** [4895] 1150–6 (1989).

[3]D. Bonn, H. Kellay, and J. Meunier, "Viscous Fingering and Related Instabilities in Complex Fluids," *Philos. Mag. B*, **78** [2] 131–42 (1998).

[4]D. Rautaray, R. Kavathekar, and M. Sastry, "Using the Dynamic, Expanding Liquid–Liquid Interface in a Hele–Shaw Cell in Crystal Growth and Nanoparticle Assembly," *Faraday Discuss*., **129**, 205 (2005).

[5]H. Schift, L. J. Heyderman, M. Auf der Maur, and J. Gobrecht, "Pattern Formation in Hot Embossing of Thin Polymer Films," *Nanotechnology*, **12**, 173–7 (2001).

[6]D. Perugini and G. Poli, "Viscous Fingering During Replenishment of Felsic Magma Chambers by Continuous Inputs of Mafic Magmas: Field Evidence and Fluid-Mechanics Experiments," *Geology*, **33** [1] 5–8 (2005).

[7]W. G. Fahrenholtz, "The ZrB_2 Volatility Diagram," *J. Am. Ceram. Soc.*, **88** [12] 3509–12 (2005).

[8]F. Monteverde and A. Bellosi, "Oxidation of ZrB_2-Based Ceramics in Dry Air," *J. Electrochem. Soc.*, **150** [11] B552–9 (2003).

[9]W. G. Fahrenholtz, "Thermodynamics of ZrB_2–SiC Oxidation: The Formation of a SiC-Depleted Region," *J. Am. Ceram. Soc.*, **90** [1] 143–8 (2007).

[10]S. R. Levine, E. J. Opila, M. C. Halbig, J. D. Kiser, M. Singh, and J. A. Salem, "Evaluation of Ultra-High Temperature Ceramics for Aeropropulsion Use," *J. Eur. Ceram. Soc.*, **22**, 2757–67 (2002).

[11]E. J. Opila, S. R. Levine, and J. Lorincz, "Oxidation of ZrB_2- and HfB_2 Based Ultra-High Temperature Ceramics: Effect of Ta Additions," *J. Mater. Sci.*, **39**, 5969–77 (2004).

[12]F. Monteverde, "The Thermal Stability in Air of Hot Pressed Diboride Matrix Composites for Uses at Ultra-High Temperatures," *Corrosion Sci.*, **47**, 2020–33 (2005).

[13]M. M. Opeka, I. G. Talmy, and J. A. Zaykoski, "Oxidation-Based Materials Selection for 2000°C+ Hypersonic Aerosurface: Theoretical Considerations and Historical Experience," *J. Mater. Sci.*, **39**, 5887–904 (2004).

[14]S. N. Karlsdottir, J. W. Halloran, F. Monteverde, and A. Bellosi, "Oxidation of ZrB2–SiC: Comparison of Furnace Heated Coupons and Self-Heated Ribbon Specimens"; *Proceedings of the International Conference on Advanced Ceramics and Composites*, Daytona Beach, FL, January 21–26, 2007 (in press).

[15]S. N. Karlsdottir, J. W. Halloran, and A. N. Grundy, "Zirconia Transport by Liquid Convection during Oxidation of Zirconium Diboride–Silicon Carbide," *J. Am. Ceram. Soc.*, (2007) (in press).

[16]R. Jabra, J. Phalippau, and J. Zarzicki, "Synthesis of Binary Glass-Forming Oxide Glasses By Hot-Pressing," *J. Non-Crystalline Solids*, **42**, 489–98 (1980).

[17]S. Fujino, C. Hwang, and R. Morinaga, "Density, Surface Tension, and Viscosity of PbO–B_2O_3–SiO_2 Glass Melts," *J. Am. Ceram. Soc.*, **87** [1] 10–6 (2004).

[18]D. M. Sciti, A. Brach, and A. Bellosi, "Long Term Oxidation Behavior and Mechanical Strength Degradation of a Pressureless Sintered ZrB_2–$MoSi_2$ Ceramic," *Scripta Mater.*, **53**, 1297–302 (2005).

[19]Y. G. Gogotsi, Y. P. Yaroshenko, and F. Porz, "Oxidation Resistance of Boron Carbide Ceramics," *J. Mater. Sci. Lett.*, **11** 308 (1992). □